Comptes Rendus

Géoscience

Sciences de la Planète

Carolina Neumann Keim and Marcos Farina

Death and taphonomy of Holocene stromatolites from Lagoa Vermelha, Brazil

Research article — Terrestrial and aquatic ecosystems

Death and taphonomy of Holocene stromatolites from Lagoa Vermelha, Brazil

Carolina Neumann Keim® *, *a* **and Marcos Farina** *a*

a Universidade Federal do Rio de Janeiro, Rio de Janeiro, RJ, Brazil

Current address: Instituto de Microbiologia Paulo de Góes, CCS, UFRJ, Av. Carlos Chagas Filho, 373, Cidade Universitária, 21941-902, Rio de Janeiro, RJ, Brazil
(C. N. Keim)

E-mails: cnkeim@micro.ufrj.br (C. N. Keim), marcos.farina.souza@gmail.com
(M. Farina)

Abstract. Stromatolites are laminated rocks, comprising both authigenic and allochthonous materials, which arise under strong influence of both microorganisms and environmental conditions. Growing stromatolites are rare nowadays, limiting our understanding on how microbial mats produce stromatolites. Stromatolites from Lagoa Vermelha in Brazil were claimed as living, lithifying structures several years ago, but recently have been reported as dead, bleached skeletons. Here we confirm that they are currently not forming new laminae. This was confirmed by the absence of the microbial mat coat, enabling colonization of exposed surfaces by barnacles, boring cyanobacteria, and burrowing metazoans, which contributed to erosion and loss of some original features while adding new, distinct biomarkers.

Keywords. Stromatolite, Lagoa Vermelha, Fossilization, Hypersaline, Fluorescence.

1. Introduction

Stromatolites are sedimentary rocks showing domal, conical, columnar or flat shapes, and laminated facies. Most of them are calcareous, comprising both authigenic and allochthonous materials in varying proportions. Stromatolites emerge from microbial mats, which are benthic microbial ecosystems found in shallow aquatic environments and tidal flats [Riding, 2000, Dupraz et al., 2009, Riding, 2011, Bosak et al., 2013, Suosaari et al., 2019]. Microbes in microbial mats arrange themselves in layers according to their physiological characteristics [Gemerden, 1993, Dupraz and Visscher, 2005, Dupraz et al., 2009]. They produce adhesive polymers able to trap solid particles, incorporating them within the microbial mat as it grows upwards towards sunlight [Riding, 2011, Bosak et al., 2013, Suosaari et al., 2019]. The interplay

---

* Corresponding author.

between microbial physiology and environmental conditions triggers the precipitation of authigenic minerals, leading to mineral precipitation within specific microenvironments within the mat, which binds loose grains together and results in the characteristic laminations [Dupraz and Visscher, 2005, Dupraz et al., 2009, Suosaari et al., 2019]. With time, the precipitation and consolidation of lamina after lamina produces stromatolites [Dupraz and Visscher, 2005, Dupraz et al., 2009, Riding, 2011, Bosak et al., 2013, Suosaari et al., 2019].

Stromatolites are very common in sedimentary settings from the Precambrian Eon, but become scarce towards the Anthropocene [Riding, 2000, 2011, Bosak et al., 2013, Suosaari et al., 2019]. Today, living stromatolites are found in a few environments, including freshwater, brackish, marine, and hypersaline environments [Reid et al., 1995, 2003, Gischler et al., 2008, Planavsky and Ginsburg, 2009, Castro-Contreras et al., 2014, Chagas et al., 2016, Zeyen et al., 2021]. Studies on living, growing stromatolites have been fundamental for the interpretation of the ancient stromatolites as fossilized microbial mats, as well as for mechanistic explanations on how microbial mats produce consolidated laminations, and how they change with diagenesis [Riding, 2011].

Several records of living stromatolites in Lagoa Vermelha in Brazil [Höhn et al., 1986, Vasconcelos et al., 2006, Spadafora et al., 2010, Vasconcelos et al., 2014] contrast with recent works reporting only bleached skeletons from 2004 on [Silva et al., 2004, Alves and Silva, 2011, Sampaio et al., 2015, Laut et al., 2017, 2019, Keim et al., 2020]. The presence of living stromatolites in Lagoa Vermelha (Rio de Janeiro State, Brazil) was first described in a scientific paper by Höhn et al. [1986]. Further work described domal stromatolites capped by 3–5 cm thick, lithifying microbial mats [Höhn et al., 1986, Vasconcelos et al., 2006]. In addition, microbial mats 2–6 cm thick were observed on sediment surfaces between 1982 and 2002 [Höhn et al., 1986, Lopes et al., 1986, Moreira et al., 1987, Elias et al., 1997, Van Lith et al., 2002, Silva et al., 2004, Silva and Carvalhal, 2005, Santelli et al., 2006]. These microbial mats contained alternating layers of whitish carbonate minerals and colored organic layers dominated by microbial phototrophs, such as cyanobacteria and purple sulfur bacteria [Vasconcelos et al., 2006]. How-

ever, a straightforward relationship between the microbial mats and the lithified laminae in stromatolites was not established. For example, pure calcite was found in the first mineral layer of the microbial mat overlying Lagoa Vermelha stromatolites [Vasconcelos et al., 2006], but not within consolidated laminae [Spadafora et al., 2010, Carvalho et al., 2018, Keim et al., 2020], which are largely composed of high Mg-calcite, very high Mg-calcite (protodolomite), and aragonite [Keim et al., 2020]. Radiocarbon analysis suggested that a stromatolite collected in Lagoa Vermelha stopped growth around 1440 ± 60 AD, but some uncertainty persists because the reservoir effect was not calculated for Lagoa Vermelha [Carvalho et al., 2018]. Such ages could indicate that the microbial mats coating Lagoa Vermelha stromatolites in 1982–2004 [Höhn et al., 1986, Elias et al., 1997, Vasconcelos et al., 2006, Spadafora et al., 2010] were not producing additional, consolidated laminae to be added to the underlying stromatolites.

In this work, we confirm that the stromatolites of Lagoa Vermelha stopped adding new laminae, analyze how and why stromatolites lose their microbial mat cap and stopped growth, and how they changed after they became naked skeletons. Because these are recent stromatolites, it is easier to unravel original and post-depositional contributions, which could help in the interpretation of the taphonomy of ancient counterparts.

2. Materials and methods

2.1. *Field description*

Lagoa Vermelha is a coastal, hypersaline lagoon in the municipality of Saquarema, Rio de Janeiro State, Brazil (Figure 1). It is separated from the Atlantic Ocean by a sandbar 200–400 m in width, from hypersaline Lagoa de Araruama by another sandbar at least 700 m wide (Figure 1b), and from freshwater Lagoa de Jacarepiá by about 2400 m (not shown). Lagoa Vermelha is small, about 4.3 km in length and at most 750 m in width [Bidegain and Bizerril, 2002], and shallow, reaching about 1.7 m in depth [Höhn et al., 1986]. The lagoon was divided into five parts by artificial sandbars (Figure 1b), and the eastern parts are currently used as evaporation ponds by an artisanal saltern at the Northeast shore.

Artificial channels bring hypersaline water from nearby Araruama Lagoon, which is eutrophic [Bidegain and Bizerril, 2002, Laut et al., 2017, 2019]. Recently, Lagoa Vermelha was considered a eutrophic environment [Laut et al., 2017, 2019, Pennafirme et al., 2019].

2.2. *Sample collection and preparation*

Biofilm and stromatolite samples were collected in Lagoa Vermelha at the south shore (22°55′58″S, 42°23′35″W) in January 18, 2013, and at the northeast shore (22°55′35″S, 42°22′09″W) in October 15, 2015 (Figure 1b). Several excursions were done in 2013–2015 for additional field work. Field work and analyses focused on the south shore, and were later confirmed by analysis of samples collected in the north shore.

In the laboratory, stromatolites were cut with a saw and sub-sampled. Small samples were cut perpendicularly to the laminations using a low-speed diamond wheel saw (South Bay Technology, INC; model 650) and hand-polished with silicon carbide sandpaper. Some were embedded in Spurr's resin (Polysciences) before polishing. For transmitted polarized light microscopy and fluorescence microscopy, samples were hand-polished with sandpaper until they became sufficiently thin, and mounted with Entellan® and coverslips. Living biofilm samples were observed in the day after they were collected.

Reflected light images of both biofilm and stromatolite samples were obtained with a Nikon AZ1000 stereomicroscope equipped with a Nikon Digital Sight DS-Ri1 camera. Several high-quality images were used to construct a high-resolution mosaic of the polished surface using the Adobe Photoshop CC 2015 software. Transmitted light microscopy images were obtained in either a Zeiss Axioplan microscope equipped with an Evolution MP 5.0 color camera (Media Cybernetics) using the Nomarski interference mode, or in a Zeiss Axioplan 2 light microscope equipped with a Color View XS digital video camera, using epi-fluorescence and crossed polarizers. Filters for epi-fluorescence were from Zeiss: (i) blue fluorescence (365 nm–420 nm), filter set 02 (488002-0000); (ii) yellow-green fluorescence (450/490–515 nm), filter set 09 (488009-0000); (iii) green fluorescence (470/20–505/530 nm), filter set 13 (488013-0000-000);

and (iv) red fluorescence (546/12–590 nm), filter set 15 (488015-0000).

For scanning electron microscopy, we used both freshly broken and polished samples. Only the broken samples were gold-sputtered using a Baltec SCD 050 equipment. Scanning electron microscopy using either secondary or backscattered electrons was done with a Jeol JSM-6490LV equipped with Noran EDS detector.

3. Results

3.1. *Observations in the field*

The temperature of the lagoon water remained between 20 and 30 °C (mean 26 °C) along 2013, 2014 and 2015, whereas salinity varied from 51 to 97‰ (average 78‰), and pH values ranged from 7.3 to 8.7 (average 8.2). Although varied, these values comply with previous observations [Höhn et al., 1986, Vasconcelos and McKenzie, 1997, Van Lith et al., 2002, Alves and Silva, 2011, Laut et al., 2017, Pennafirme et al., 2019].

Lagoon water varied from clear and transparent to green and turbid (Figure 2a,b). We found several stromatolites removed from their original places in the lagoon, and deposited at the shore (Figure 2a,c,d), whereas those not so easily accessed by people remained in their original places (Figure 2e,f). During field work, we have never observed stromatolites coated by cm-thick microbial mats as described previously [Höhn et al., 1986, Vasconcelos et al., 2006, 2014]. Instead, they alternated between (i) completely naked, bleached mineral surfaces (Figure 2c,e); (ii) a very thin, green slimy coat (figure 2c,d); and (iii) a soft olive-green biofilm, measuring 1–2 mm in thickness (Figure 2f). The presence of barnacle shells on most stromatolite skeleton outer surfaces, including the upper convex surfaces (Figure 2c), indicate that these mineral surfaces had been exposed to lagoon water for some time before we began fieldwork in January 2013.

The lagoon bottom alternated between light grey exposed sediment minerals (not shown) and the millimeter-thick biofilm coat, which also coated the stromatolites (Figure 2f). This biofilm was soft and easily displaced from hard surfaces, turning into loose flocs. It was observed at depths up to ~1 m in Lagoa Vermelha. Microbial mats 1–3 cm thick were observed only at the north shore of Lagoa Vermelha,

Figure 1. Satellite images showing the localization of Lagoa Vermelha in Brazil. (a) Part of Rio de Janeiro State in Brazil showing the location of Lagoa Vermelha along the coast (rectangle). (b) Area enclosed by the rectangle in (a) showing Lagoa Vermelha, part of nearby Lagoa de Araruama, and the Atlantic Ocean. Asterisks show the places where samples were collected. Images obtained with the software ArcGISEarth.

in an area lacking both domal stromatolites and laminated crusts.

Light microscopy showed that the biofilm coating stromatolites on October 15, 2015 was composed predominantly by diatoms, fecal pellets, foraminifera and ostracods (Figure 3a–c). Several species of microcrustaceans grazed around (e.g. Figure 3d). Figure 3e shows the main species of foraminifera. In addition, rare filaments of cyanobacteria (Figure 3b,f,g) and gliding colorless sulfur bacteria, probably *Beggiatoa* sp. (Figure 3f), were observed. The paucity of filamentous microbes and their remains could explain the weak cohesiveness observed in this biofilm [for the roles of filamentous microorganisms in cohesiveness and textures of biofilms and microbial mats,

see for example the work of Gerdes et al., 2000]. Local variations in biofilm composition were common (for example, compare Figure 3a,b,f,g). Thick, laminated microbial mats were observed only on a tidal flat at the North shore of Lagoa Vermelha and in the nearby salt evaporation artificial ponds (not shown).

3.2. *Stromatolite structure and taphonomy*

Figure 4 shows the surface of the sagittal plane of a Lagoa Vermelha stromatolite. Laminated facies predominate at the core, whereas clotted facies appear at the top, the bottom, and the periphery. Some cm-wide voids are also present. Burrows 0.7–1.0 mm wide are widespread on peripheral regions, but not

Figure 2. Photographs of Lagoa Vermelha and stromatolites. (a,b) Lagoa Vermelha landscapes at the South shore. (a) Picture taken on January 18, 2013, showing clear water and several stromatolites at the shore, displaced from their original places. (b) Picture taken on October 13, 2014, showing green, turbid water due to excess phytoplankton. (c) Dry stromatolites at the South shore, showing abundant barnacle shells attached to outer surfaces. For scale, each individual barnacle shell is about 1 cm wide. (d) Broken stromatolite found at the shore. Wet surfaces show green color, contrasting with the almost white color of dry mineral surfaces. (e,f) Stromatolites observed in their original places. (e) Image taken on October 13, 2014, at the east border. Partially broken stromatolite heads are seen above the water level due to an exceptionally dry year. Each stromatolite is about 40 cm in diameter. (f) Underwater photograph taken close to the South border on October 15, 2015, showing a thick (1–2 mm) green-to-brown biofilm coating the lagoon bottom, including the stromatolite. This individual stromatolite is about 30 cm in diameter.

in the laminated core. The occurrence of a well-laminated core and thrombolitic portions at the base and the top of Lagoa Vermelha stromatolites suggests a changing environment in the timescale of stroma-tolite growth, as proposed by Carvalho et al. [2018] based on radiocarbon age determination.

The stromatolite core showed millimeter-thick, convex, parallel laminae, showing shade variations,
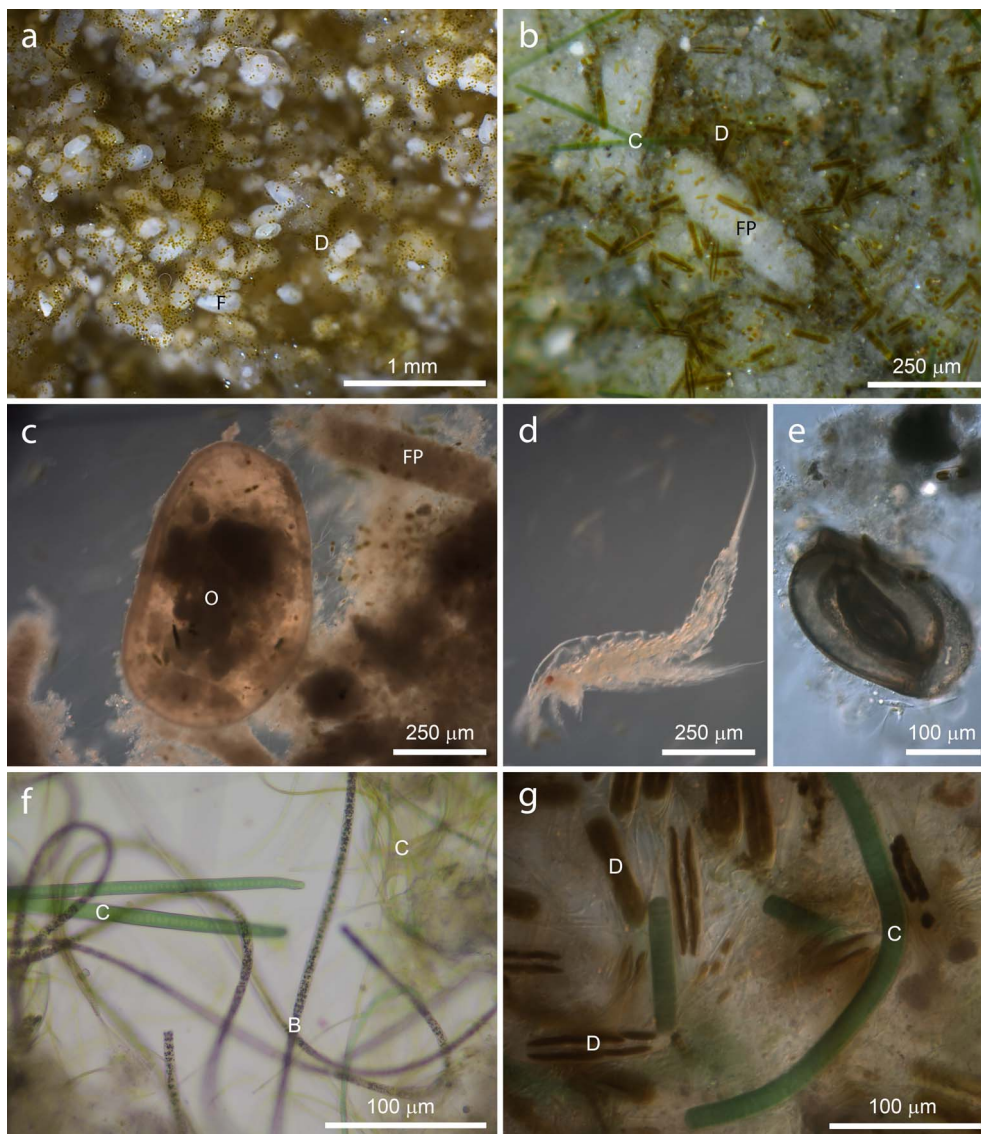
Figure 3. Light micrographs of the millimeter-thick biofilm coating stromatolites on October 13, 2014. (a) Sample consisting mainly of diatoms (olive green dots, D) and foraminifera (white, oblong, F). (b) Diatoms (olive green rods, D) and filamentous cyanobacteria (C) along with abundant fecal pellets (white rods, FP). (c) Fecal pellets (FP) and remains of an ostracod (O). (d) Example of microcrustacean that grazed on the biofilms. (e) Remains of a foraminifera. (f) At least two distinct species of filamentous cyanobacteria (C) along with colorless sulfur bacteria (B for *Beggiatoa*). (g) High magnification showing diatoms (D) and filamentous cyanobacteria (C). (a,b) Stereomicroscopy, reflected light. (c–g) Nomarski interference contrast, transmitted light.

sometimes separated by empty voids (Figure 5a). Color variations could be observed in both laminated and clotted regions (Figure 5a–d) and indicate differences in composition and/or texture as observed previously [Keim et al., 2020]. Extensive regions of both laminated and clotted regions consisted of rather
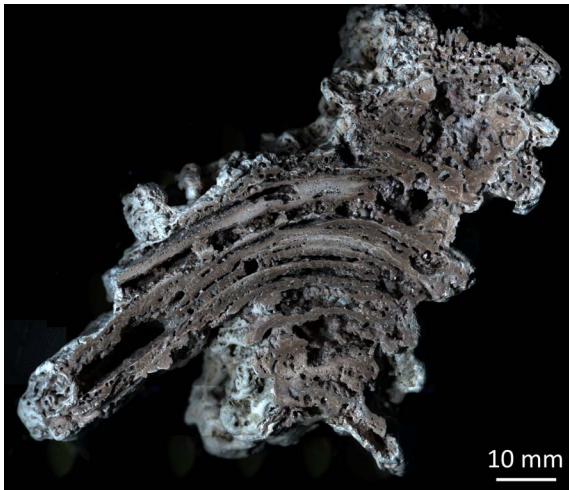
Figure 4. Stromatolite from Lagoa Vermelha (reflected light microscopy, mosaic). Note the laminated facies in the core, and clotted facies on both top and bottom. Circular burrows, about 1 mm in diameter, occur at peripheral regions, specially at the top right corner.

irregular peloids cemented together (Figure 5b), contrasting with the regular size and shape of fecal pellets (Figure 5d).

Fecal pellets were found mostly in the outer regions, where they were cemented within metazoan burrows and other surfaces (Figure 5d) as observed before [Keim et al., 2020]. The peripheral regions contained metazoan burrows, 0.7–1.0 mm wide, reaching up to 1 cm from the outer surface (Figure 5c). Gastropod, bivalve, ostracod and foraminifera shells were found both on the surfaces and embedded in the stromatolite fabric, but were more common in the voids between laminae (Figure 5e,f), indicating that most of them arrived after laminae consolidation. Previous work found the same types of shells within Lagoa Vermelha stromatolites [Silva et al., 2004, Spadafora et al., 2010, Keim et al., 2020]. Silva et al. [2004] identified most gastropods as *Hydrobia*, most ostracods as *Cyprideis*, and the main bivalve species as *Anomalocadia brasiliana*. Inorganic clastic materials were rare and consisted mainly of quartz (Figure 5e). A thin mineral layer coated many surfaces, including laminae, peloids, fecal pellets, shells and metazoan burrows (Figure 5b–f). This mineral coat seems to be responsible for cementing most

peloids, fecal pellets and shells to the stromatolite fabric as proposed before [Keim et al., 2020].

Figure 6 shows the minerals coating a small gastropod shell found in a stromatolite. The texture of the coat was similar within and outside the shell (Figure 6a), as well as in the surrounding areas. In either transmitted or reflected light microscopy images, or in scanning electron microscopy, this mineral coat was 5–100 µm wide. In both foraminifera and gastropods, the coat was slightly thinner on the inner shell surface as compared to the outer surface (Figure 6a). Figure 6b shows minerals arranged in bunches on the mineral fringe, as well as filamentous microorganisms, diatom frustules, and EPS remains in what appears to be additional layers deposited onto the mineral fringe coating the shell. Higher magnification showed the mineral bunch at the top to be composed of long, thin minerals with trigonal symmetry, sometimes presenting a hole in the center suggesting a hollow head (Figure 6c). The proximity with an EPS mass could suggest a role of EPS in nucleation, although the underlying carbonates are probable nucleating sites as well. The mineral bunch at the bottom in Figure 6b consisted of thin rhombohedral plates with the acute angles pointing outwards (Figure 6d). Both morphologies have been observed before in Lagoa Vermelha stromatolites [Spadafora et al., 2010], and very similar shapes have been found in freshwater stromatolites [Castro-Contreras et al., 2014], low Mg-calcite minerals from a coastal hypersaline microbial mat [Perri et al., 2018], in an ancient reef [Cabioch et al., 1999], and also in soil extracts [Párraga et al., 2004]. Thus, these seem to be features common in authigenic Ca–Mg carbonates.

Polarized light microscopy showed that the minerals in stromatolites were largely birefringent (Figure 7a,c,e), as described before [Spadafora et al., 2010, Keim et al., 2020]. Fluorescence microscopy put on evidence otherwise hidden features, which may be interpreted as organic matter and remains of microorganisms (Figure 7b,d,f). As a general finding, bright areas in the polarized light image showed the weakest fluorescence, indicating that these areas are poor in organics as compared to surrounding areas. Conversely, weakly birefringent areas showed the strongest fluorescence (Figure 7). Observation of several samples using polarized light and SEM suggests that the weak birefringence would be due to reduced sizes of Ca–Mg carbonate crystals, which is the
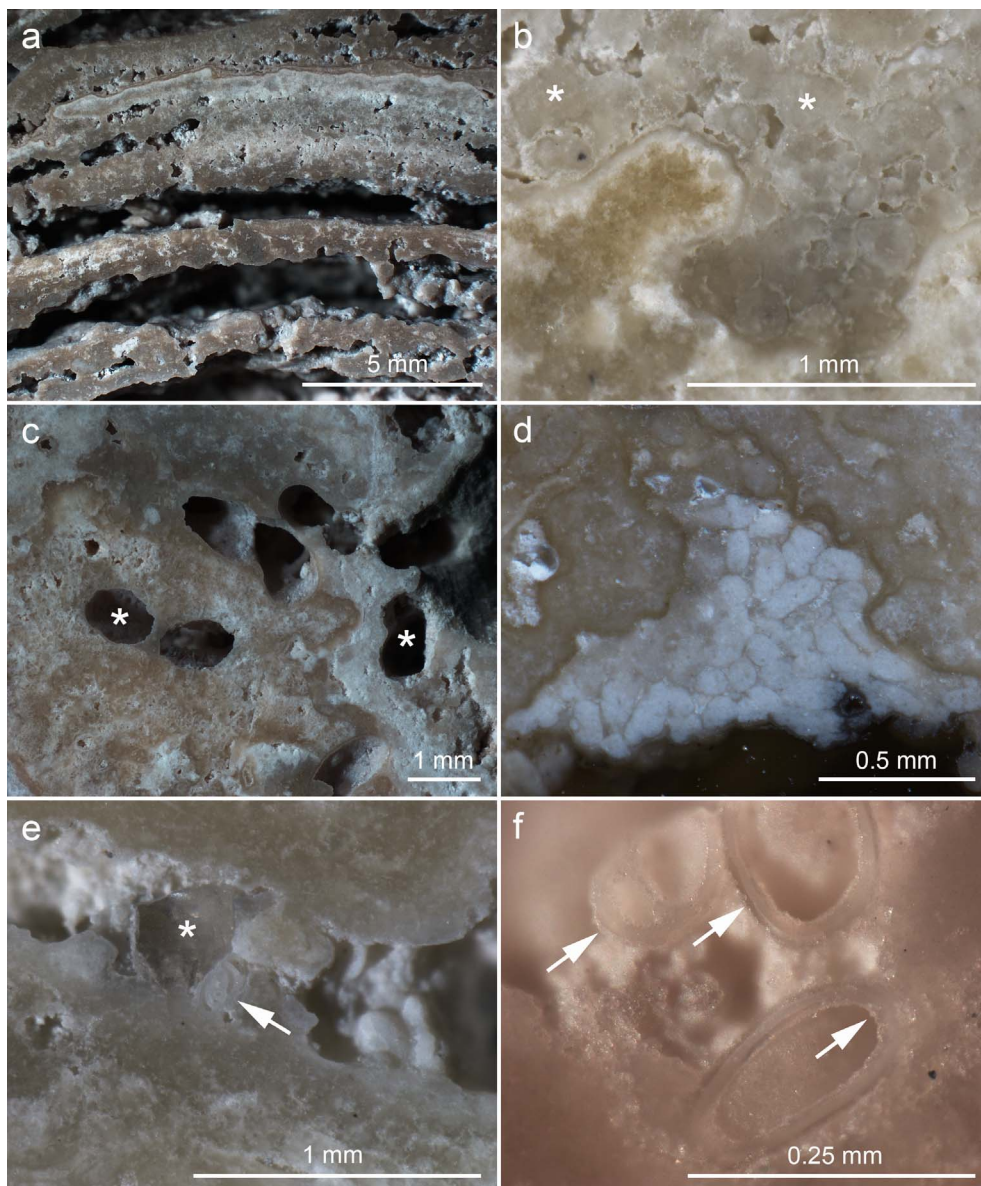
Figure 5. Reflected light stereomicroscopic images of polished stromatolite surfaces. (a) Laminated facies in the stromatolite core. (b) Clotted region showing abundant peloids (asterisks) cemented together by a thin mineral layer. (c) Holes consisting of metazoan burrows (asterisks). (d) Cluster of fecal pellets cemented to the stromatolite (white rods). (e) Space between two laminae containing a quartz grain (asterisk) and a foraminifera shell (arrow). (f) Cluster of foraminifera shells with both inner and outer surfaces coated by a thin mineral layer, which cements them to the stromatolite surface (arrows).

predominant minerals in Lagoa Vermelha stromatolites [Keim et al., 2020].

Most features fluoresced green and yellow (Figures 7, 8), in contrast to weaker and more specific

blue (not shown) and red fluorescence (Figure 8). The strongest birefringence and lowest fluorescence were observed in the radial mineral fringe coating several surfaces (Figure 7a–d). Considering birefringence as
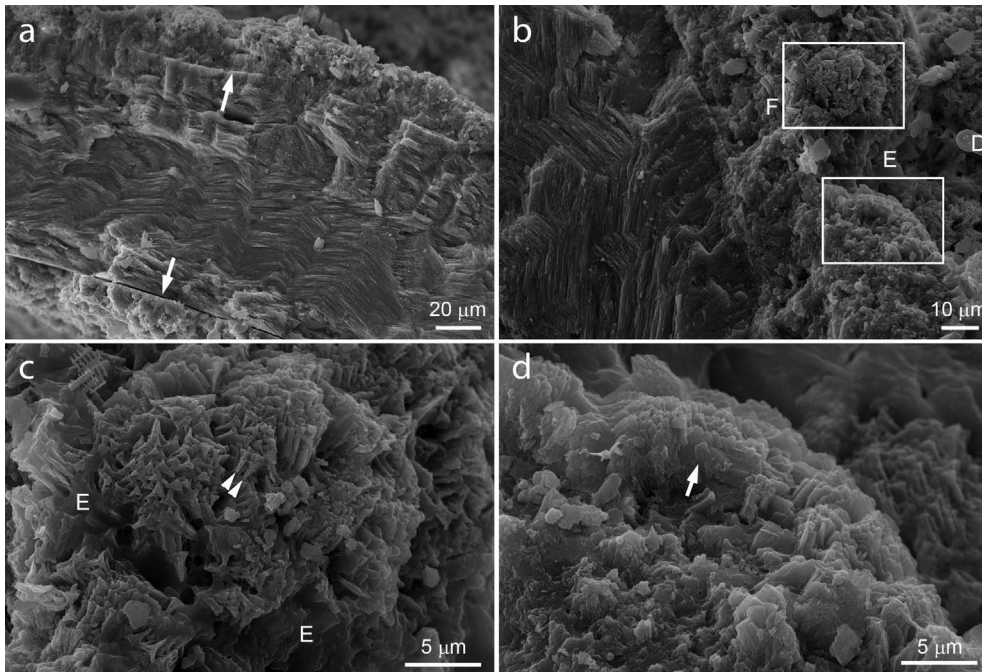
Figure 6. Scanning electron micrographs of freshly broken stromatolite surfaces, showing minerals grown onto a gastropod shell. (a) Broken gastropod shell showing mineral fringes growing both inside (bottom arrow) and outside (top arrow) of the shell. Note that the fringe is wider on the outer shell surface (top) than on the inner surface (bottom). (b) Larger magnification of the top of the shell showing the mineral fringe in detail, along with a filamentous prokaryote (F), a diatom frustule (D), and EPS (E). Boxed areas are enlarged in (c, d). (c) Larger magnification of the region enclosed in the upper rectangle in (b) showing thin crystals growing from the EPS underneath (E). Side view of the crystals show they are long and thin, with enlarged tops (arrowheads). Top view shows triangular tops with small holes in the center. (d) Larger magnification of the region enclosed in the bottom rectangle in (b) showing rhombohedral plates growing radially, with the acute angles pointing upwards (arrow). Secondary electrons, 25 kV.

a proxy for Ca–Mg carbonates and fluorescence as a proxy for organic materials, these images indicate that the fringe consists largely of minerals growing radially from available mineral surfaces, with little (if any) contribution of organic materials. Both light microscopy techniques show that in some places the fringe coating inner stromatolite surfaces is composed by at least two layers (Figure 7a–d), which indicate that the fringe precipitated intermittently.

Figure 7a,b show highly fluorescent, poorly birefringent circular profiles cemented to stromatolite surfaces by the mineral fringe. Their rather regular shape and size indicate that they consist of fecal pellets. In addition, highly fluorescent spots occurred within small voids (Figure 7a,b). Shapes include rods,

cocci, and filaments, indicating that these could represent fresh remains of microbial cells. Figure 7c,d show bioclasts displaying fluorescence levels and patterns similar to the laminae, with no evidence of organic remains from the original organisms inside most of them. Bright spots showing size and shape compatible with microbial cells are abundant in poorly birefringent areas (Figure 7c,d). Comparison of fluorescence levels of Figures 7b and d indicate that these could represent aged cell remains.

In Figure 7e,f, the remains of several well-preserved, mineralized, filamentous microorganisms can be recognized by their conspicuous morphology. They show birefringence and fluorescence levels similar to the surrounding minerals, indicating
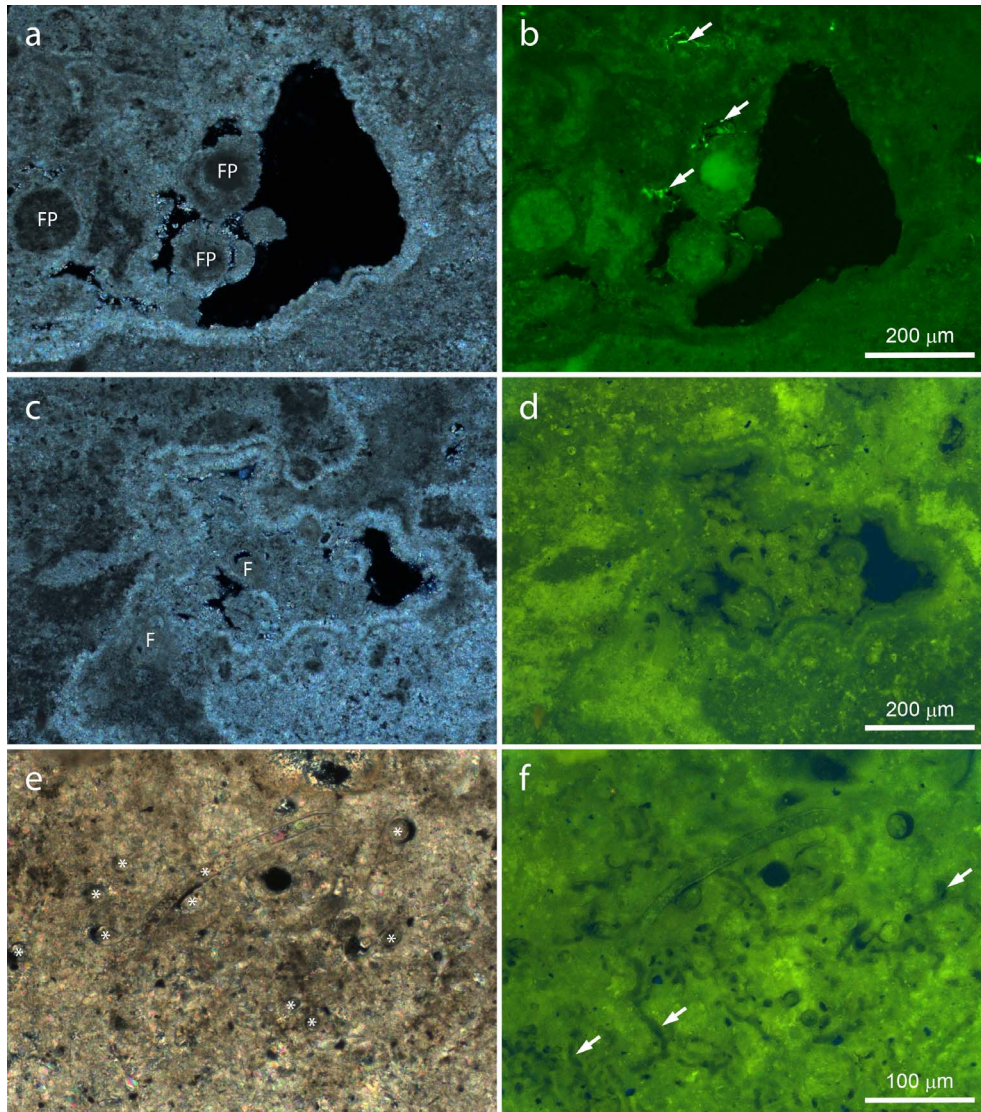
Figure 7. Polished slices of stromatolite observed by polarized and fluorescence light microscopy. Note the inverse brightness of polarized light (a,c,e) and fluorescence images (b,d,f). (a,b) Border area showing heterogeneous birefringence and fluorescence, as well as weakly birefringent, highly fluorescent, well-delimited areas probably consisting of fecal pellets (FP). Note the bright fluorescent spots within small voids (arrows). Highly birefringent, weakly fluorescent mineral fringes coat all surfaces, cementing the putative fecal pellets to the stromatolite. (c,d) Void in a laminated region filled by clastic materials. Highly fluorescent, weakly birefringent regions are intercalated by weakly fluorescent, highly birefringent areas. The mineral fringe coats all surfaces, showing a single layer lining the clasts, including foraminifera shells (F), and a double layer coating stromatolite mineral surfaces. Fluorescence is stronger in small spots, corresponding to dark areas in the polarized light image. (e,f) Fossilized filamentous microorganisms (asterisks) and microscopic tubules (arrows).
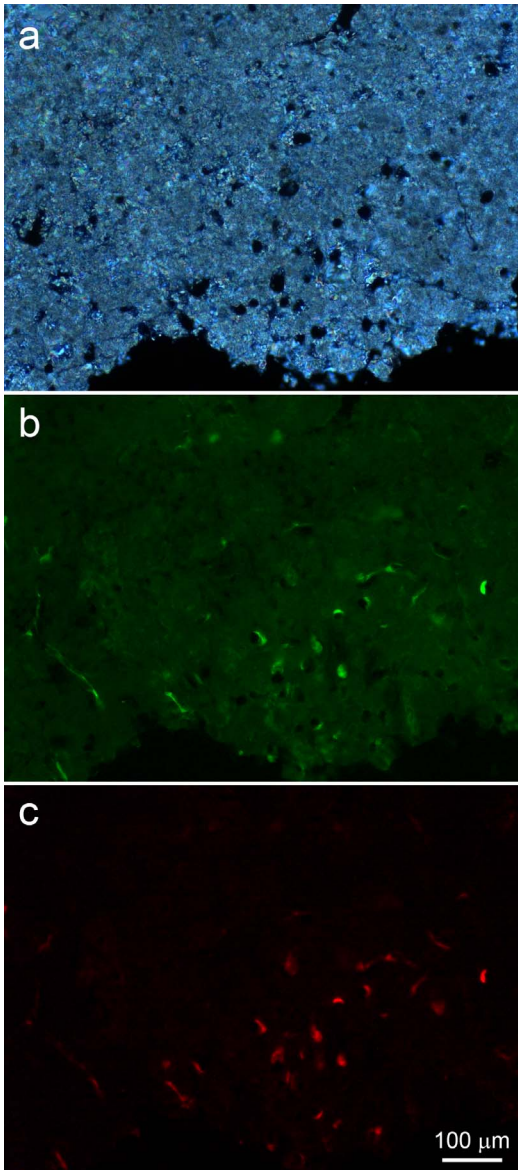
Figure 8. Polarized light microscopy (a) and fluorescence microscopy (b,c) of a thin, polished sample of a peripheral stromatolite region. (a) Border area showing abundant microscopic tubules. (b) Highly fluorescent spots juxtaposed to tubule walls and filaments running on the bottom left are probably due to remains of microorganisms that thrived within the tubules. A weak, heterogeneous and widespread green fluorescence is also observed. (c) The strong red fluorescence co-localized with the green fluorescence within tubules and in the filaments at the left is compatible with that of the photosynthesis pigment chlorophyll.

that carbonate minerals largely substituted the original cell materials, whereas fluorescent organic remains were lost and/or distributed around. Circular holes are observed in both polarized and fluorescent light images (Figure 7e,f), but presumably empty tubular holes parallel to the plane of the sample are particularly evident in the fluorescent light image, where they appear darker than their surroundings (Figure 7f).

Comparison of polarized and fluorescence light images shows strong birefringence and weak autofluorescence in the minerals around such tubules (Figure 8a,b). Fluorescence microscopy showed many of them partially filled with strongly autofluorescent materials, which would probably correspond to remains from the microorganisms that inhabited the tubules (Figure 8b,c). Their autofluorescence is strong in yellow, green and red. In particular, the red autofluorescence (Figure 8c) is compatible with the autofluorescence of the photosynthesis pigment chlorophyll, indicating that these could be remains of cyanobacteria.

Accordingly, scanning electron microscopy showed the remains of filamentous microorganisms within microscopic tubules (Figure 9a,b). Figure 9a shows several of them at the border of a stromatolite, some still containing the organic remains of filamentous microorganisms. Their organic nature could be identified due to the translucent character at the scanning electron microscope when using backscattered electrons (Figure 9a). In other samples, filaments remaining within the tubules were brittle, indicating that their organic remains were largely substituted for minerals (Figure 9b), as observed by light microscopy in Figure 7e,f. Their shapes suggest that they were filamentous microorganisms (Figure 9b). In samples embedded in resin, the outlines of stromatolite laminae are more evident. Figure 9c shows a site at the outer surface dominated by microscopic tubules. They are more concentrated towards the surface, as observed in Figure 9a. Some entombed remains of microorganisms could be observed, but they did not seem related to the nearby tubules (Figure 9c) and may represent microbial remains from the time minerals in this lamina were precipitated, as previously described in similar environments [e.g. Gischler et al., 2008, Couradeau et al., 2013, Castro-Contreras et al., 2014, Perri et al., 2018, Shiraishi et al., 2020, Debrie et al., 2022].
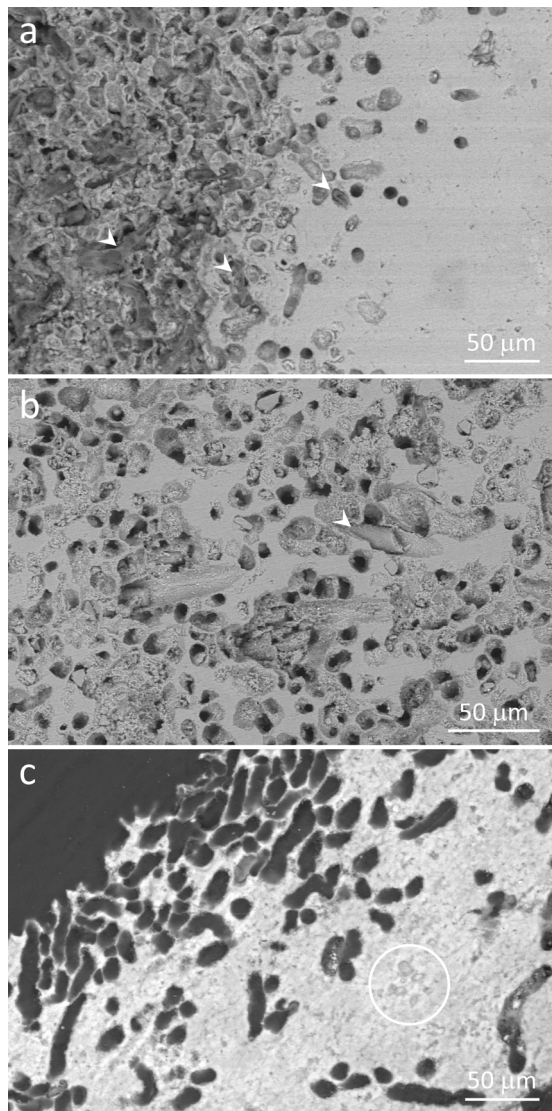
Figures 7e,f, 8 and 9a,b show both fresh and mineralized filamentous microorganism remains within tubules. Their size, shape, probable presence of chlorophyll, habitat, and proximity with outer surfaces (Figures 8 and 9a,c) indicate that they consisted of remains of filamentous cyanobacteria which lived within the stromatolite minerals. The green, thin slime observed on some wet stromatolite surfaces in the field (Figure 2d), the strong autofluorescence observed within the tubules (Figure 8), and the organic character observed by SEM (Figure 9a) indicate that some of them were still alive at the time the samples were collected. Even though red fluorescence was not observed in the brittle, mineralized boring microfossils shown in Figures 7e,f and 9b, their size, shape and habitat are similar to the fresh ones observed in Figures 8 and 9a, suggesting that they were cyanobacteria as well.

Figure S1 (Supplementary Material) presents several reflected light and scanning electron micrographs taken from a stromatolite slab, ranging from the millimeter to the micrometer scale. It shows that the tubules observed in Figures 7e,f, 8 and 9 occur only close to stromatolite borders, usually not exceeding 500 µm from the outer surface, and are completely absent from the inner laminae (Figure S1a–c). At the mm-scale, the outer borders enriched in tubules seem smoother as compared to inner surfaces, which showed more kinks (Figure S1a–c). At the micrometer scale, several stretches of outer borders are dominated by the tubules (Figure 9a,c; Figure S1), which could explain the smoother appearance at low magnification. Such differences between inner and outer surfaces indicate that the tubules would be associated to corrosion of stromatolite outer surfaces, which would not occur in inner surfaces.

Figure 9. Scanning electron micrographs of polished stromatolite samples showing peripheral regions containing abundant microscopic tubules, some still harboring filamentous microorganisms. (a) Image showing both polished (right) and the original stromatolite surface, which consists largely of openings of the tubules (left). Note abundant organic remains of filamentous microorganisms, some still filling the tubules (arrowheads). Their translucent appearance is due to the organic nature. (b) Abundant tubules in a peripheral area, some harboring fossilized, brittle, filamentous microorganisms (arrowhead).

The activities of cyanobacteria can have strong influence on the carbonate minerals in stromatolites, leading to either precipitation or dissolution of minerals. Those cyanobacteria involved in mineral precipitation usually increase the pH in the nearby microenvironment during photosynthesis leading to increased supersaturation, and/or produce abundant EPS where minerals are nucleated and grow [Dupraz and Visscher, 2005, Dupraz et al., 2009]. Accordingly, mineral precipitation around cyanobacteria it is relatively common, specially onto secreted EPS, generating characteristic textures and/or mineral composition [Gischler et al., 2008, Couradeau et al., 2013, Castro-Contreras et al., 2014, Perri et al., 2018, Shiraishi et al., 2020, Debrie et al., 2022]. On the other hand, some cyanobacteria burrow into carbonate minerals, pumping Ca^{2+} ions through their cells to decrease saturation in the area of contact of the apical cell with the mineral. Localized undersaturation induce mineral dissolution in the microborings inhabited by these cyanobacteria [Garcia-Pichel et al., 2010, Guida and Garcia-Pichel, 2016]. Microboring cyanobacteria are widespread in carbonate minerals from marine habitats, including microbialites [Golubic, 1969, Campion-Alsumard et al., 1996, Perry, 1998, Macintyre et al., 2000, Reid and Macintyre, 2000, Arp et al., 2003, Reid et al., 2003, Pantazidou et al., 2006, Planavsky and Ginsburg, 2009, Duguid et al., 2010, Radtke and Golubic, 2011, Wyness et al., 2022].

Based on the distribution of tubules only close to outer surfaces of the stromatolites (Figure S1), on the presence of organic, autofluorescent remains or fossilized cells inside some of the tubules (Figures 7e,f, 8, 9a,b), on the difference in texture and relief between inner and outer stromatolite surfaces (Figure S1), and on the absence of any structural or compositional relation between tubules, microorganisms inhabiting them, and the surrounding minerals (Figures 9 and S1), we interpreted these micrometer-wide tubes as microborings, and the cyanobacteria inhabiting them as microboring cyanobacteria.

This implies that under some environmental conditions, boring cyanobacteria grow and bore into illuminated areas of Lagoa Vermelha stromatolites, leading to mineral dissolution. When environmental conditions change, their dead, soft bodies can be replaced by minerals, leading to fossilization. Thus, they could act both in dissolution and precipitation

of minerals close to the stromatolite surfaces, depending if they are alive or dead, as well as on the environmental conditions.

4. Discussion

4.1. *Life and death of stromatolites from Lagoa Vermelha*

Field work confirmed that the cm-thick microbial mats coating stromatolites were lost. Instead, Lagoa Vermelha stromatolites were intermittently coated by a thin microbial coat, 1–2 mm in thickness, containing diatoms as main phototrophs (Figure 3). In contrast, the microbial mats that once coated Lagoa Vermelha stromatolites included two green layers dominated by cyanobacteria (*Gloeocapsa*, *Spirulina* and *Microcoleus* species), along with a purple layer dominated by purple sulfur bacteria (e.g. *Thiocystis* sp.) and a layer enriched in Ca–Mg carbonates [Vasconcelos et al., 2006]. In the biofilm, the birefringence characteristic of carbonates is concentrated in cylindrical fecal pellets and in the shells of foraminifera and ostracods, whereas in microbial mats collected at the north border of Lagoa Vermelha, carbonates are observed mainly in irregular to rounded "microoncoids" about 0.2–1.0 mm in diameter [Guedes et al., 2022]. Cylindrical fecal pellets were observed on stromatolite outer surfaces and burrows (Figure 5d) but not in the laminated core, whereas the peloids observed in the stromatolite fabric present irregular shapes [Figure 5(b); Keim et al., 2020] rather similar to the "microoncoids" observed by Guedes et al. [2022]. Indeed, a previous work proposed that these peloids within Lagoa Vermelha stromatolites originated from sequential precipitation of authigenic minerals, with bioclasts observed mainly close to voids [Keim et al., 2020]. Thus, we consider that this biofilm did not participate in the genesis of new stromatolite laminae. Perhaps, under the appropriate conditions, this biofilm may develop into a lithifying microbial mat able to produce additional stromatolitic laminae.

In the stromatolites of Lagoa Vermelha, we observed barnacle shells only at the outer surfaces, whereas cyanobacteria microborings and metazoan burrows reached at most 500 μm and 10 mm into the stromatolite, respectively. Bioerosion and barnacle shells were never observed deep into the

stromatolite core. It seems that the stromatolite's mineral surfaces were protected from those animals and microorganisms during growth by the microbial mat coat, consisting of a thick web of microorganisms, exopolysacharides and dead cell materials. Once the stromatolites lost their microbial mats, colonization by barnacles, burrowing metazoans, and boring microorganisms could occur on the exposed mineral surfaces, but this biota could not reach the stromatolite core because they thrive close to the outer surface. The absence of the thick microbial mat coating the stromatolites described before [Höhn et al., 1986, Vasconcelos et al., 2006, 2014], the inconsistency of the thin biofilms with the stromatolite cores, the presence of barnacle shells only at the outer surfaces, and the finding of both metazoan and microorganism borings only close to outer surfaces indicate that these stromatolites are not adding new mineral laminae to their tops, and have been "dead" for a while before they were collected in January 2013.

Thin mineral fringes, consisting of a palisade of coarse crystals, were observed coating several surfaces, including laminae, shells, peloids, and also the walls of some metazoan burrows. Spadafora et al. [2010] and Keim et al. [2020] also observed such fringes in Lagoa Vermelha stromatolites and considered that they precipitated directly from water onto available carbonate mineral surfaces. Observation of banding in some of these mineral coats indicate stepwise mineral deposition, which could be related to climate cycles in Lagoa Vermelha. Because metazoan burrows occurred after the microbial mat coat has been lost, and some presented these mineral fringes, precipitation of such fringes probably continued after loss of the microbial mat coat, resulting from abiotic processes as proposed previously [Spadafora et al., 2010, Keim et al., 2020]. The olive-green biofilms that grew intermittently onto outer stromatolite surfaces would not participate in precipitation of these mineral fringes, since the fringes were equivalent in inner and outer surfaces, whereas the biofilm grew only onto external surfaces.

As discussed above, Lagoa Vermelha stromatolites lost their thick microbial mat coats some time ago. The high turbidity and green color of the water observed in the field provide a clue that eutrophication could be the cause. Indeed, previous work suggested that Lagoa Vermelha is currently eutrophic [Laut et al., 2017, 2019, Pennafirme et al., 2019]. Recurrent episodes of high turbidity due to excess phytoplankton, which is a characteristic of eutrophic environments, could have led phototrophs in the microbial mats on the stromatolites to death due to insufficient light. Since phototrophs are the base of the food web in microbial mats, their death could lead to the collapse of microbial mats. Thus, eutrophication could explain the death of the microbial mats that once coated Lagoa Vermelha stromatolites.

In nearby Araruama Lagoon, which is hypersaline and eutrophic but much larger than Lagoa Vermelha, eutrophication changed the ecosystem metabolism from net heterotrophic, benthic-dominated, and limited by phosphorus in 1993–1995, to net autotrophic, planktonic-dominated in 2017 [Knoppers et al., 1996, Cotovicz et al., 2021]. In Araruama Lagoon, increased photosynthesis in phytoplankton driven by eutrophication consumes most of the dissolved inorganic carbon (DIC) and modulates alkalinity, decreasing the saturation state and the amount of precipitated $CaCO_3$ [Cotovicz et al., 2021]. Similarly, increased photosynthesis in the water column due to eutrophication could interfere with $CaCO_3$ precipitation in Lagoa Vermelha, including the stromatolites.

Figure 10 summarizes the findings and interpretations of the present work relative to living beings. In addition to the biologically-driven changes, climate-driven episodes of low water level could lead cyanobacteria, barnacles and burrowing metazoans to death by increased salinity or desiccation. Such conditions could also drive increased Ca–Mg carbonate precipitation, which could entomb boring cyanobacteria, add new layers to the mineral fringe, and/or cement fecal pellets and other bioclasts to some stromatolite surfaces, particularly within metazoan burrows.

5. Conclusions

Lagoa Vermelha stromatolites are currently not capped by microbial mats, nor adding new laminae to the top. Eutrophication leading to periods of excess phytoplankton and high turbidity of the water seems to be the probable cause of death of the thick
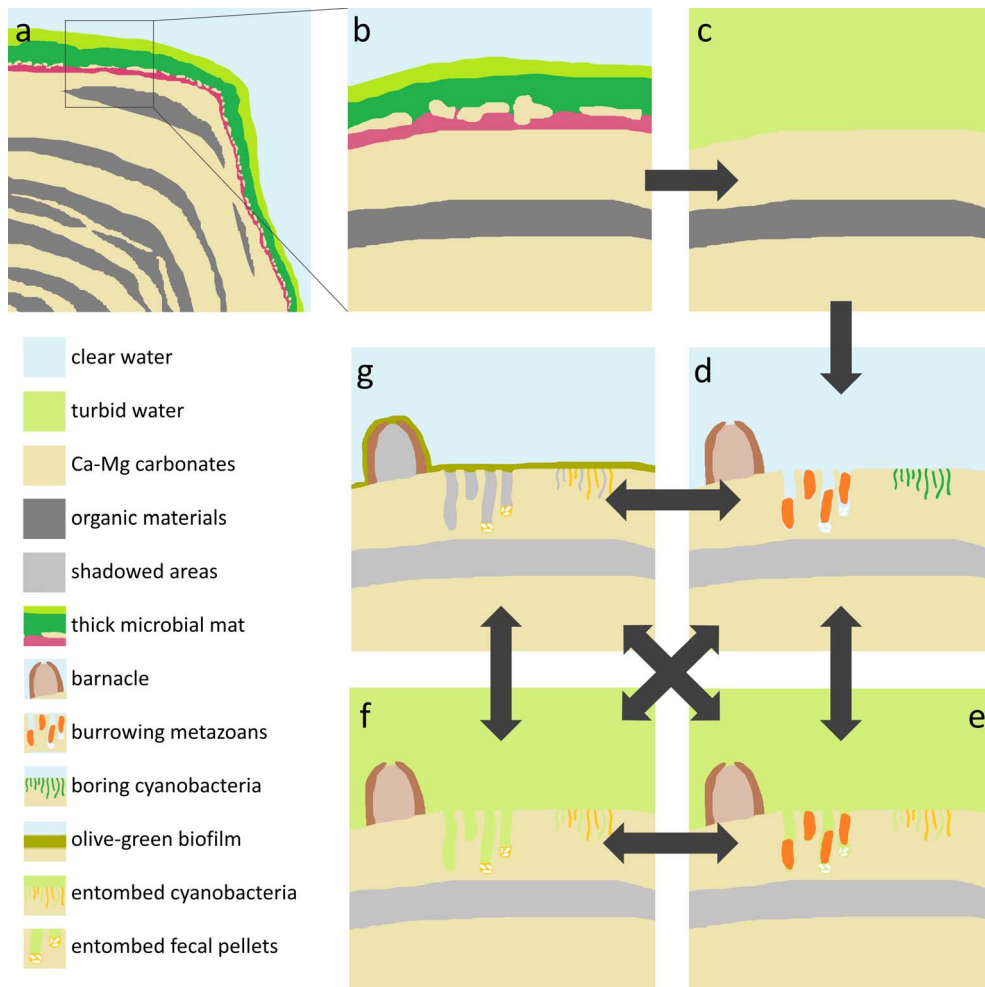
Figure 10. Model of Lagoa Vermelha stromatolites and their post-deposition changes driven by eutrophication and the biota. (a) Scheme of a growing stromatolite coated by a cm-thick, multilayered microbial mat. (b) Close-up of the top of the stromatolite, showing two green layers and a purple layer, along with an incipient mineral lamina in between. Water is clear, enabling photosynthesis up to several mm deep in the microbial mat. (c) Eutrophication drives phytoplankton blooms, which makes the water turbid. The microbial mat collapses due to the insufficient light, exposing the naked skeletons. (d) The exposed mineral surfaces become colonized by barnacles, burrowing metazoans, and boring cyanobacteria. (e) High turbidity due to phytoplankton blooms, desiccation, virus infection etc. could lead boring cyanobacteria to death, resulting in entombed filaments or empty microborings. (f) Eventually the boring metazoans die or move away, leaving fecal pellets, which can be cemented to stromatolite surfaces, particularly within the burrows. (g) During periods of clear water, a thin, olive-green, loose biofilm grows on illuminated surfaces. This biofilm is enriched in diatoms, foraminifera and fecal pellets and could contribute with additional bioclasts to the stromatolite. (d–g, arrows) Recurrence of phytoplankton blooms lead to collapse of the olive-green biofilm, leaving naked stromatolite surfaces available to be colonized by barnacles, burrowing metazoans, and cyanobacteria, which can die or move away. These steps can repeat several times, in different orders.

microbial mats previously reported on the top of the stromatolites.

The thin, olive-green biofilm coat that sometimes coats the stromatolites shows no incipient mineral laminae and is enriched in diatoms, fecal pellets, foraminifera and ostracods, whereas the core of Lagoa Vermelha stromatolites is largely formed by peloids, with little contributions of foraminifera and ostracod shells [Keim et al., 2020], and no fecal pellets. Thus, the olive-green biofilm probably does not contribute with new laminae to the stromatolites.

The presence of barnacle shells, borings and microborings only close to outer surfaces suggest that barnacles, boring metazoans, and boring cyanobacteria colonized the stromatolite mineral surfaces only after they were devoid of mats and exposed to lagoon water. Thus, they are regarded here as postdepositional changes. In addition, the presence of a mineral fringe lining some borings suggest that the stromatolite skeletons remained naked for some time before we began field work on January 2013.

The precipitation of the mineral fringe lining stromatolite surfaces and cementing bioclasts seems to be independent of the presence of a microbial mat, but result largely from supersaturation of lagoon water with respect to Ca–Mg carbonates.

Conflicts of interest

Authors have no conflict of interest to declare.

Supplementary data

Supporting information for this article is available on the journal's website under https://doi.org/10.5802/crgeos.201 or from the author.

References

Alves, S. A. P. M. N. and Silva, L. H. S. (2011). Estudo dos estromatólitos biscuit da Lagoa Vermelha (Rio de Janeiro – Brasil). *Rev. Geol.*, 24, 94–107. http://www.periodicos.ufc.br/geologia/article/view/1402.

Arp, G., Reimer, A., and Reitner, J. (2003). Microbialite formation in seawater of increased alkalinity, Satonda Crater Lake, Indonesia. *J. Sediment. Res.*, 73, 105–127.

Bidegain, P. and Bizerril, C. (2002). *Lagoa de Araruama - Perfil Ambiental do Maior Ecossistema Lagunar Hipersalino do Mundo*. Semads, Rio de Janeiro, Brazil.

Bosak, T., Knoll, A. H., and Petroff, A. P. (2013). The meaning of stromatolites. *Annu. Rev. Earth Planet. Sci.*, 41, 21–44.

Cabioch, G., Taylor, F. W., Corrège, T., Rècy, J., Edwards, L. R., Burr, G. S., Le Cornec, F., and Banks, K. A. (1999). Occurrence and significance of microbialites in the uplifted Tasmaloum reef (SW Espiritu Santo, SW Pacific). *Sediment. Geol.*, 126, 305–316.

Campion-Alsumard, T., Golubic, S., and Pantazidou, A. (1996). On the euendolithic genus *Solentia* Ercegovic (Cyanophyta/Cyanobacteria). *Algol. Stud.*, 83, 107–127.

Carvalho, C., Oliveira, M., Macario, K., Guimarães, R., Keim, C., Sabadini-Santos, E., and Crapez, M. (2018). Stromatolite growth in Lagoa Vermelha, southeastern coast of Brazil: evidence of environmental changes. *Radiocarbon*, 60, 383–393.

Castro-Contreras, S. I., Gingras, M. K., Pecoits, E., Aubet, N. R., Petrash, D., Castro-Contreras, S. M., Dick, G., Planavsky, N., and Konhauser, K. O. (2014). Textural and geochemical features of freshwater microbialites from Laguna Bacalar, Quintana Roo, Mexico. *Palaios*, 29, 192–209.

Chagas, A. A. P., Webb, G. E., Burne, R. V., and Southam, G. (2016). Modern lacustrine microbialites: towards a synthesis of aqueous and carbonate geochemistry and mineralogy. *Earth-Sci. Rev.*, 162, 338–363.

Cotovicz, L. C., Knoppers, B. A., Régis, C. R., Tremmel, D., Costa-Santos, S., and Abril, G. (2021). Eutrophication overcoming carbonate precipitation in a tropical hypersaline coastal lagoon acting as

a CO_2 sink (Araruama Lagoon, SE Brazil). *Biogeochemistry*, 156, 231–254.

Couradeau, E., Benzerara, K., Gérard, E., Estève, I., Moreira, D., Tavera, R., and López-García, P. (2013). Cyanobacterial calcification in modern microbialites at the submicrometer scale. *Biogeosciences*, 10, 5255–5266.

Debrie, J., Prêt, D., Menguy, N., Estève, I., Sans-Jofre, P., Saint Martin, J. P., and Benzerara, K. (2022). Mapping mineralogical heterogeneities at the nm-scale by scanning electron microscopy in modern Sardinian stromatolites: Deciphering the origin of their laminations. *Chem. Geol.*, 609, article no. 121059.

Duguid, S. M. A., Kyser, T. K., James, N. P., and Rankey, E. C. (2010). Microbes and ooids. *J. Sediment. Res.*, 80, 236–251.

Dupraz, C., Reid, R. P., Braissant, O., Decho, A. W., Norman, R. S., and Visscher, P. T. (2009). Processes of carbonate precipitation in modern microbial mats. *Earth-Sci. Rev.*, 96, 141–162.

Dupraz, C. and Visscher, P. T. (2005). Microbial lithification in marine stromatolites and hypersaline mats. *Trends Microbiol.*, 13, 429–438.

Elias, V. O., de Barros, A. M. A., de Barros, A. B., Simoneit, B. R. T., and Cardoso, J. N. (1997). Sesquiterpenoids in sediments of a hypersaline lagoon: a possible algal origin. *Org. Geochem.*, 26, 721–730.

Garcia-Pichel, F., Ramírez-Reinat, E., and Gao, Q. (2010). Microbial excavation of solid carbonates powered by P-type ATPase-mediated transcellular Ca^{2+} transport. *Proc. Natl. Acad. Sci. USA*, 107, 21749–21754.

Gemerden, H. (1993). Microbial mats: a joint venture. *Mar. Geol.*, 113, 3–25.

Gerdes, G., Klenke, T., and Noffke, N. (2000). Microbial signatures in peritidal siliciclastic sediments: a catalogue. *Sedimentology*, 47, 279–308.

Gischler, E., Gibson, M. A., and Oschmann, W. (2008). Giant holocene freshwater microbialites, Laguna Bacalar, Quintana Roo, Mexico. *Sedimentology*, 55, 1293–1309.

Golubic, S. (1969). Distribution, taxonomy, and boring patterns of marine endolithic algae. *Am. Zool.*, 9, 747–751.

Guedes, C. B., Arena, M. C., Santos, H. N., Valle, B., Santos, J. A., Favoreto, J., and Borghi, L. (2022). Sedimentological and geochemical characteriza-tion of microbial mats from Lagoa Vermelha (Rio de Janeiro, Brazil). *J. Sediment. Res.*, 92, 591–600.

Guida, B. S. and Garcia-Pichel, F. (2016). Extreme cellular adaptations and cell differentiation required by a cyanobacterium for carbonate excavation. *Proc. Natl. Acad. Sci. USA*, 113, 5712–5717.

Höhn, A., Tobschall, H. J., and Maddock, J. E. L. (1986). Biogeochemistry of a hypersaline lagoon east of Rio de Janeiro, Brazil. *Sci. Total Environ.*, 58, 175–185.

Keim, C. N., Santos, H. N., Santiago, C. S., Pennafirme, S., Neumann, R., Schnellrath, J., Lima, I., Crapez, M. A. C., and Farina, M. (2020). Microstructure and mineral composition of Holocene stromatolites from Lagoa Vermelha, a hypersaline lagoon in Brazil: insights into laminae genesis. *J. Sediment. Res.*, 90, 887–905.

Knoppers, B., Souza, W. F. L., Souza, M. F. L., Rodriguez, E. G., Landim, E. F. C. V., and Vieira, A. R. (1996). In situ measurements of benthic primary production, respiration and nutrient fluxes in a hypersaline coastal lagoon of SE Brazil. *Rev. Bras. Oceanogr.*, 44, 155–165.

Laut, L., Figueiredo, M. S. L., Lorini, M. L., Belart, P., Clemente, I., Martins, M. V. A., Mendonça Filho, J. G., and Laut, V. M. (2019). Diatoms from the most hypersaline lagoon in Brazil: Vermelha Lagoon. *Cont. Shelf Res.*, 181, 111–123.

Laut, L., Martins, M. V. A., Frontalini, F., Ballalai, J. M., Belart, P., Habib, R., Fontana, L. F., Clemente, I. M. M. M., Lorini, M. L., Mendonça Filho, J. G., Laut, V. M., and Figueiredo, M. S. L. (2017). Assessment of the trophic state of a hypersaline-carbonatic environment: Vermelha Lagoon (Brazil). *PLoS One*, 12, article no. e0184819.

Lopes, C. E. A., Teixeira, A. C. D., Maddock, J. E. L., Tobschall, H. J., and Höhn, A. (1986). Absorption of metals by benthic microbial mats and sediments of Lagoa Vermelha, Brazil. *Sci. Total Environ.*, 58, 55–62.

Macintyre, I. G., Prufert-Bebout, L., and Reid, R. P. (2000). The role of endolithic cyanobacteria in the formation of lithified laminae in Bahamian stromatolites. *Sedimentology*, 47, 915–921.

Moreira, I., Patchineelam, R., and Rebello, A. L. (1987). Preliminary investigations on the occurrence of diagenetic dolomite in surface sediments of Lagoa Vermelha, Brazil. *GeoJournal*, 14, 357–360.

Pantazidou, A., Louvrou, I., and Economou-Amilli, A. (2006). Euendolithic shell-boring cyanobacteria and chlorophytes from the saline lagoon Ahivadolimni on Milos Island, Greece. *Eur. J. Phycol.*, 41, 189–200.

Párraga, J., Rivadeneyra, M. A., Martín-García, J. M., Delgado, R., and Delgado, G. (2004). Precipitation of carbonates by bacteria from a saline soil, in natural and artificial soil extracts. *Geomicrobiol. J.*, 21, 55–66.

Pennafirme, S., Pereira, D. C., Pedrosa, L. G. M., Machado, A. S., Silva, G. O. A., Keim, C. N., Lima, I., Lopes, R. T., Paixão, I. C. N. P., and Crapez, M. A. C. (2019). Characterization of microbial mats and halophilic virus-like particles in a eutrophic hypersaline lagoon (Vermelha Lagoon, RJ, Brazil). *Reg. Stud. Mar. Sci.*, 31, article no. 100769.

Perri, E., Tucker, M. E., Słowakiewicz, M., Whitaker, F., Bowen, L., and Perrotta, I. D. (2018). Carbonate and silicate biomineralization in a hypersaline microbial mat (Mesaieed sabkha, Qatar): roles of bacteria, extracellular polymeric substances and viruses. *Sedimentology*, 65, 1213–1245.

Perry, C. T. (1998). Grain susceptibility to the effects of microboring: implications for the preservation of skeletal carbonates. *Sedimentology*, 45, 39–51.

Planavsky, N. and Ginsburg, R. N. (2009). Taphonomy of modern marine Bahamian microbialites. *Palaios*, 24, 5–17.

Radtke, G. and Golubic, S. (2011). Microbial euendolithic assemblages and microborings in intertidal and shallow marine habitats: insight in cyanobacterial speciation. In *Advances in Stromatolite Geobiology*, volume 131 of *Lecture Notes in Earth Sciences*, pages 233–263. Springer, Berlin, Heidelberg.

Reid, R. P., James, N. P., Macintyre, I. G., Dupraz, C. P., and Burne, R. V. (2003). Shark Bay stromatolites: microfabrics and reinterpretation of origins. *Facies*, 49, 299–324.

Reid, R. P. and Macintyre, I. G. (2000). Microboring versus recrystallization: further insight into the micritization process. *J. Sediment. Res.*, 70, 24–28.

Reid, R. P., Macintyre, I. G., Browne, K. M., Steneck, R. S., and Miller, T. (1995). Modern marine stromatolites in the Exuma Cays, Bahamas: uncommonly common. *Facies*, 33, 1–18.

Riding, R. (2000). Microbial carbonates: the geological record of calcified bacterial-algal mats and biofilms. *Sedimentology*, 47(suppl. 1), 179–214.

Riding, R. (2011). The nature of stromatolites: 3,500 million years of history and a century of research. In Reitner, J., Quéric, N.-V., and Arp, G. J., editors, *Advances in Stromatolite Geobiology*, volume 131 of *Lecture Notes in Earth Sciences*, pages 29–74. Springer, Berlin, Heidelberg.

Sampaio, L. F., Dal' Bó, P. F. F., and Borghi, L. (2015). Morphology and genesis of microbially induced sedimentary structures (MISS) in sediments of the Lagoa Vermelha (Região dos Lagos – Rio de Janeiro). *Anu. Inst. Geociên. – UFRJ*, 38, 95–106.

Santelli, R. L., Wagener, A. L. R., Wagener, K., and Patchineelam, S. (2006). Assessing past environmental changes through sediment records in a hypersaline lagoon. *Croat. Chem. Acta*, 79, 129–141. https://hrcak.srce.hr/2623.

Shiraishi, F., Omori, T., Tomioka, N., Motai, S., Suga, H., and Takahashi, Y. (2020). Characteristics of $CaCO_3$ nucleated around cyanobacteria: implications for calcification process. *Geochim. Cosmochim. Acta*, 285, 55–69.

Silva, L. H. S. and Carvalhal, S. B. V. (2005). Biolaminóides calcários holocênicos da Lagoa Vermelha, Brasil. *Anu. Inst. Geociên. – UFRJ*, 28, 59–70.

Silva, L. H. S., Senra, M. C. E., Faruolo, T. C. L. M., Carvalhal, S. B. V., Alves, S. A. P. M. N., Damazio, C. M., Shimizu, V. T. A., Santos, R. C., and Iespa, A. A. C. (2004). Composição paleobiológica e tipos morfológicos das construções estromatolíticas da Lagoa Vermelha, RJ, Brazil. *Rev. Brasil. Paleontol.*, 7, 193–198. https://www.sbpbrasil.org/revista/edicoes/7_2/silvacomp.pdf.

Spadafora, A., Perri, E., McKenzie, J. A., and Vasconcelos, C. (2010). Microbial biomineralization processes forming modern Ca:Mg carbonate stromatolites. *Sedimentology*, 57, 27–40.

Suosaari, E. P., Reid, R. P., and Andres, M. S. (2019). Stromatolites, so what?! A tribute to Robert N. Ginsburg. *Depositional Rec.*, 5, 486–497.

Van Lith, Y., Vasconcelos, C., Warthmann, R., Martins, J. C. F., and McKenzie, J. A. (2002). Bacterial sulfate reduction and salinity: two controls on dolomite precipitation in Lagoa Vermelha and Brejo do Espinho (Brazil). *Hydrobiologia*, 485, 35–49.

Vasconcelos, C., Dittrich, M., and McKenzie, J. A. (2014). Evidence of microbiocoenosis in the formation of laminae in modern stromatolites. *Facies*, 60, 3–13.

Vasconcelos, C. and McKenzie, J. A. (1997). Microbial mediation of modern dolomite precipitation and diagenesis under anoxic conditions (Lagoa Vermelha, Rio de Janeiro, Brazil). *J. Sediment. Res.*, 67, 378–390.

Vasconcelos, C., Warthmann, R., McKenzie, J. A., Visscher, P. T., Bittermann, A. G., and Van Lith, Y. (2006). Lithifying microbial mats in Lagoa Vermelha, Brazil: modern precambrian relics? *Sediment. Geol.*, 185, 175–183.

Wyness, A. J., Roush, D., and McQuaid, C. D. (2022). Global distribution and diversity of marine euendolithic cyanobacteria. *J. Phycol.*, 58, 746–759.

Zeyen, N., Benzerara, K., Beyssac, O., Daval, D., Muller, E., Thomazo, C., Tavera, R., López-García, P., Moreira, D., and Duprat, E. (2021). Integrative analysis of the mineralogical and chemical composition of modern microbialites from ten Mexican lakes: what do we learn about their formation? *Geochim. Cosmochim. Acta*, 305, 148–184.